Roles of the tensor and pairing correlations on the halo formation in ^{11}Li

Takayuki Myo[1], Kiyoshi Katō[2], Hiroshi Toki[1] and Kiyomi Ikeda[3]
[1] *Research Center for Nuclear Physics (RCNP), Osaka University, Ibaraki, Osaka 567-0047, Japan,*
[2] *Division of Physics, Graduate School of Science, Hokkaido University, Sapporo 060-0810, Japan,*
[3] *The Institute of Physical and Chemical Research (RIKEN), Wako, Saitama 351-0198, Japan.*

1 Introduction

The tensor force is an essential component in nuclear force and plays an important role in the nuclear structure. The exact calculations clarified that the contribution of the tensor force is comparable to the central case in the light nuclei. It is important to understand the effect of the tensor force on the nuclear structure. In this study, we investigate the role of the tensor correlation in the neutron-halo nuclei ^{11}Li, and their neighboring nuclei.

A pioneering secondary-beam experiment found that the size of ^{11}Li was surprisingly large, which was outside of the common sense of Nuclear Physics [1]. This large size was later interpreted as due to the halo structure of two neutrons around the ^{9}Li core nucleus [2]. This finding together with others motivated the nuclear physics community to start a new research field for the study of unstable nuclei and built new facilities of Radioactive Ion Beams (RIB) in several laboratories as RIKEN, MSU, GSI, GANIL and others. Many experimental findings were shown later for ^{11}Li: a) The halo neutrons have almost equal amount of the s-wave component with respect to the p-wave component [3]. b) The $E1$ strength distribution has a large enhancement near the threshold [4]. c) The charge radius is larger than that of ^{9}Li [5].

The biggest puzzle from the theory side is the large s-wave component for the halo neutrons. If we interpret this fact in the shell model, the shell gap at $N = 8$ has to disappear. However, no theory can explain this disappearance and all the theoretical works for ^{11}Li and neighboring nuclei had to accept that the $1s_{1/2}$ state is brought down to the $0p_{1/2}$ state without knowing its reason[7, 8]. It is therefore the real challenge for theoretician to understand this disappearance of the $N = 8$ shell gap, to be called s-p shell gap problem, which is worked out in this paper by developing a framework to treat the tensor force explicitly in the nucleon-nucleon interaction.

The tensor force plays an important role in the nuclear structure. For example, the contribution of the tensor force in the binding of ^{4}He is comparable to that of the central force[10, 11]. The tensor correlation induced by the tensor force was demonstrated important for the ^{4}He+n system [12, 13, 14]. In our recent study [16], we developed a theoretical framework of the tensor-optimized shell model to treat the tensor force in the shell model basis explicitly including $2p$-$2h$ excitations. We found that the $(0s_{1/2})^{-2}(0p_{1/2})^{2}$ excitation of proton-neutron pair has a special importance in describing the tensor correlation in ^{4}He [15, 14, 16]. In the ^{4}He+n system, because this $2p$-$2h$ excitation receives the strong Pauli-blocking from the last neutron occupying the $p_{1/2}$-orbit, a considerable amount of the $p_{1/2}$-$p_{3/2}$ splitting in ^{5}He is reproduced [14]. This Pauli-blocking effect from the $p_{1/2}$-orbit caused by the tensor force should be present also for ^{11}Li.

Hence, it is very interesting to study the effect of the tensor correlation together with the pairing correlation for the s-p shell gap problem in ^{11}Li. This is the purpose of this paper. To this end, we shall perform the configuration mixing based on the shell model framework for ^{9}Li to describe the tensor and pairing correlations explicitly. In particular, we pay attention to the special features of the tensor correlation. For ^{11}Li, we shall solve the configuration mixing of the ^{9}Li+n+n problem which treats both correlations, and investigate further the Coulomb breakup strength of ^{11}Li and other observables to see the effect of these correlations.

2 Model

We shall begin with the introduction of the model for ^{9}Li, whose Hamiltonian is given as

$$H(^{9}\mathrm{Li}) \;=\; \sum_{i=1}^{9} t_i - t_G + \sum_{i<j} v_{ij} \ . \tag{1}$$

Here, t_i, t_G, and v_{ij} are the kinetic energy of each nucleon, the center-of-mass term and the two-body NN interaction consisting of central, spin-orbit, tensor and Coulomb terms, respectively. The wave function of ^{9}Li$(3/2^{-})$ is described in the tensor-optimized shell model[16]. We express ^{9}Li by a multi-configuration $\Psi(^{9}\mathrm{Li}) = \sum_i a_i \, \Phi_i^{3/2^-}(b_\alpha)$, where we consider up to the $2p$-$2h$ excitations within the $0p$ shell for $\Phi_i^{3/2^-}$ in a shell model type wave function. Here, we adopt the spatially modified harmonic oscillator wave function (Gaussian function)

as a single particle orbit and treat the length parameters b_α of every orbit α of $0s$, $0p_{1/2}$ and $0p_{3/2}$ as variational parameters. This is important to optimize the tensor correlation[14, 16]. We solve the variational equation for the Hamiltonian of ^{9}Li and determine $\{a_i\}$ and the length parameters of three orbits.

For ^{11}Li, the Hamiltonian of ^{9}Li+n+n is given as

$$H(^{11}\mathrm{Li}) = H(^9\mathrm{Li}) + \sum_{i=1}^{3} T_i - T_G + \sum_{i=1}^{2} V_{cn,i} + V_{nn}, \tag{2}$$

where $H(^9\mathrm{Li})$, T_i and T_G are the internal Hamiltonian of ^{9}Li given by Eq. (1), the kinetic energies of each cluster and the center-of-mass of the three-body system, respectively. The wave function of ^{11}Li with the spin J is given as

$$\Psi^J(^{11}\mathrm{Li}) \quad = \quad \sum_i \mathcal{A}\left\{ [\Phi_i^{3/2^-}, \chi_i^j(nn)]^J \right\}, \tag{3}$$

where j is the spin of the last two neutrons. We obtain coupled differential equations for the two neutron wave functions χ by using the orthogonality condition model[6, 9] to treat the antisymmetrization in Eq. (2), which provides the Pauli-blocking effect caused by the two neutrons. Here, we keep the length parameters b_α of the single particle wave functions as those obtained for ^{9}Li. We describe the two neutron wave functions precisely in a few-body approach of the hybrid-TV model[6, 9]. The radial part of the relative wave functions are expanded with a finite number of Gaussian bases centered at the origin.

We shall fix now the interactions defined in Hamiltonians in Eqs. (1) and (2). We should first of all remind that we take into account the tensor force in the shell model basis explicitly as the first time. On the other hand, the short range repulsion has to be taken into account in the effective interaction, which is not yet available. Hence, we have to construct carefully the interactions in the Hamiltonian. We base therefore on the effective interaction GA$'$ for v_{ij} in Eq. (1), which has explicitly the tensor force applying the AV8$'$ realistic potential from the G-matrix theory and the short range repulsion is treated in the Brueckner method[17, 18]. Then, we have to adjust the central force to avoid the double counting due to the tensor force, which is done by changing the second range of the central force by reducing the strength by 21.5% and increasing the range by 0.19 fm to reproduce the observed binding energy and the matter radius of ^{9}Li in the same manner of Refs. [14, 16].

The ^{9}Li-n potential, V_{cn}, in Eq. (2) is given by folding the MHN interaction, which has only the central force and used frequently for light nuclei [20, 21]. For the ^{9}Li+n system, the folding potential produces the proper energy splittings in the ^{10}Li spectra [9], such as 1^+–2^+ for the $p_{1/2}$-neutron, and 1^-–2^- for the $s_{1/2}$-neutron from the coupling between spins of the last neutron and ^{9}Li($3/2^-$). Furthermore, considering the small one-neutron-separation energy of ^{9}Li, we improve the tail behavior of the potential by adding a phenomenological Yukawa type potential to the original folding one[9]. Any state-dependence is not used in the ^{9}Li-n potential, such as a deep potential for the s-wave. We have to introduce one parameter, δ in the ^{9}Li-n potential to adjust the strength of the second range of the folding potential to avoid the double counting due to the explicit treatment of the tensor force[9]. This parameter is determined to reproduce the two-neutron-separation energy of ^{11}Li as 0.31 MeV after working out the tensor and the pairing correlation effects. For the potential V_{nn} of the last two neutrons in Eq. (2), we take an AV8$'$ potential.

In principle, we can work out a large space to include the full effect of the tensor force by taking $2p$-$2h$ states with very high angular momenta[16]. In order to avoid large computational efforts without loss of the physical importance in the result, we restrict the $2p$-$2h$ shell model states within the p-wave states for the description of ^{9}Li with the single Gaussian basis. We have studied that the superposition of the Gaussian bases improves the description of the spatial shrinkage for the particle states caused by the tensor correlation[16]. Using this method, so-called the Gaussian expansion method (GEM)[19], the particle-hole excitations induced by the tensor force increase and converges[16]. In the present study, we adopt the 50% enhanced tensor matrix elements with a single Gaussian bases in order to simulate the GEM effect.

3 Results

We show first the results of ^{9}Li. In Fig. 1, we display the energy surface of ^{9}Li as functions of the length parameters of two $0p$ orbits, where b_{0s} is already optimized as 1.45 fm. There are two energy minima, (a) and (b), which have almost a common $b_{0p_{3/2}}$ value of 1.7-1.8 fm, and small (0.85 fm) and large (1.8 fm) $b_{0p_{1/2}}$ values, respectively. The properties of two minima are listed in Table 1 with the dominant $2p$-$2h$ configurations and their probabilities. It is found that the minimum (a) shows a large tensor contribution, while the minimum (b) does not. Among the $2p$-$2h$ configurations, the largest probabilities are given by $(0s)^{-2}_{10}(0p_{1/2})^2_{10}$ for (a), similar to the results in Ref. [14, 16], and $(0p_{3/2})^{-2}_{01}(0p_{1/2})^2_{01}$, namely the $0p$ shell pairing correlation for (b). These

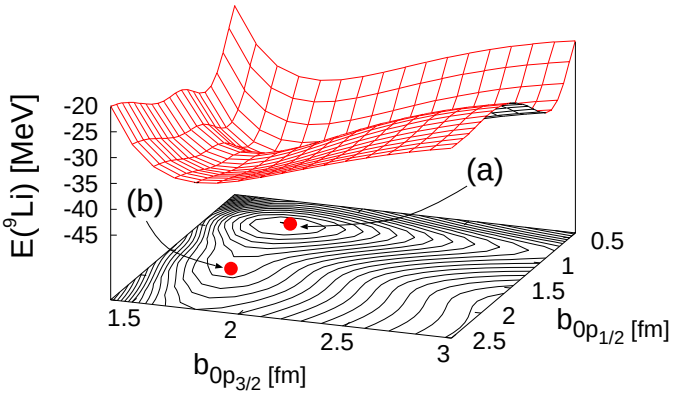

Figure 1: Energy surface of ^{9}Li with respect to the length parameters b_α of $0p$ orbits. The two minima indicated by (a) and (b) in the contour map correspond to the states due to the tensor correlation and the paring correlation, respectively.

Table 1: Properties of ^{9}Li with configuration mixing.

	Present			Expt.
	(a)	(b)	(c)	
E [MeV]	-43.8	-37.3	-45.3	-45.3
$\langle V_T \rangle$ [MeV]	-22.6	-1.8	-20.7	—
R_m [fm]	2.30	2.32	2.31	2.32±0.02[22]
$0p$-$0h$	91.2	60.1	82.9	—
$(0p_{3/2})^{-2}_{01}(0p_{1/2})^2_{01}$	0.03	37.1	9.0	—
$(0s_{1/2})^{-2}_{10}(0p_{1/2})^2_{10}$	8.2	1.8	7.2	—

results indicate that the minima (a) and (b) represent the different correlations of tensor and pairing characters, respectively. The spatial properties are also different from each other; the tensor correlation is optimized with spatially shrunk excited nucleons for (a) and the pairing correlation is optimized when two $0p$ orbits make a large spatial overlap for (b). In Table 1, we show the results of the superposition of minima (a) and (b), named as (c), to obtain a ^{9}Li wave function including the tensor and pairing correlations, simultaneously. For (c), the favored two configurations in each minimum (a) and (b) are still mixed with the $0p$-$0h$ one, and the property of the tensor correlation is kept in (c). The superposed ^{9}Li wave function possesses both the tensor and pairing correlations.

We discuss here the Pauli-blocking effect in ^{11}Li as shown in Fig. 2. For the ^{9}Li ground state (GS), in addition to the $0p$-$0h$ state, $2p$-$2h$ states caused by the tensor and pairing correlations are strongly mixed (upper panel). Let us add two neutrons more to ^{9}Li. When two neutrons occupy the $0p_{1/2}$-orbit (middle panel), the $2p$-$2h$ excitations of the tensor and pairing correlations in ^{9}Li are Pauli-blocked, simultaneously[9]. Accordingly, the correlation energy of ^{9}Li is partially lost inside ^{11}Li. For the $(1s)^2$ case of two neutrons (lower panel) the Pauli-blocking does not occur and ^{9}Li gains its correlation energy fully by the configuration mixing with the $2p$-$2h$ excitations. Hence, the relative energy distance between $(0p)^2$ and $(1s)^2$ configurations of ^{11}Li is expected to become small to break the magicity in ^{11}Li.

We perform the coupled three-body calculation of ^{11}Li considering tensor and pairing correlations fully, named as "Present". In order to see the individual effects of the tensor and paring correlations, we consider other three models of ^{11}Li with different descriptions of ^{9}Li. "Inert core" is only the $0p$-$0h$ configuration of ^{9}Li. "Tensor" and "Pairing" are the ones in which the minimum (a) and (b) in Table 1 are adopted for ^{9}Li, respectively. For each model, we determine the parameter δ in the ^{9}Li-n potential, shown in Table 2.

In Fig. 3, "Present" is found to give a large amount of the $(1s)^2$ probability $P(s^2)$, 46.9% for the last two neutrons and a large matter radius R_m, 3.41 fm for ^{11}Li, which are enough to explain the observations. The probabilities of $(p_{1/2})^2$, $(p_{3/2})^2$, $(d_{5/2})^2$ and $(d_{3/2})^2$ for the last two neutrons are obtained as 42.7%, 2.5%, 4.1% and 1.9%, respectively. This model successfully reproduces -17.4 fm of a scattering length for the 2^- state of the ^{9}Li+n system as a signature of a virtual s-state. In Fig. 3, when we individually consider the tensor and pairing correlations for ^{9}Li, $P(s^2)$ is larger for the tensor case than for the pairing case. This means that the blocking effect from the tensor correlation is stronger than the pairing case. Finally their coupling moreover

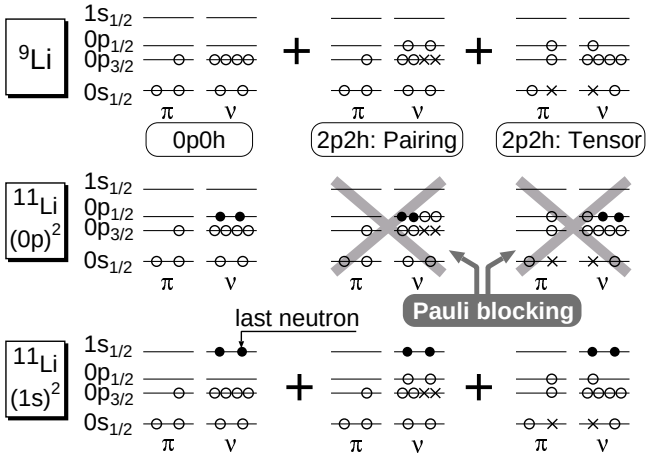

Figure 2: Schematic illustration for the Pauli-blocking in ^{11}Li. Details are described in the text.

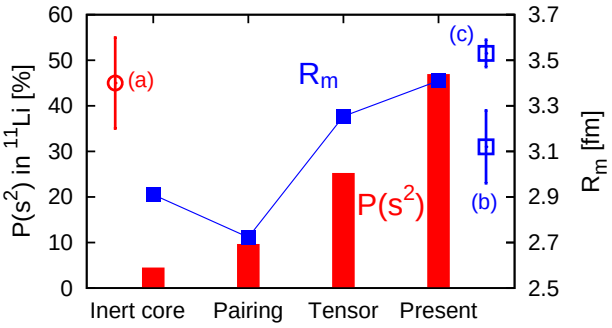

Figure 3: $(1s)^2$ probability $P(s^2)$ and matter radius R_m of ^{11}Li with four models in comparison with the experiments ((a)[3], (b)[22] and (c)[23]). The scale of $P(s^2)$ (R_m) is right (left) hand side.

Table 2: δ and the energy differences ΔE in MeV.

	Inert core	Pairing	Tensor	Present
δ	0.066	0.143	0.1502	0.1745
ΔE	2.1	1.4	0.5	-0.1

enhances $P(s^2)$ and provide the equal amount of $(1s)^2$ and $(0p)^2$ configurations. Hence, two correlations play important roles to break the magicity and make the halo structure for ^{11}Li.

In Table 2, we estimate the relative energy difference ΔE between $(1s)^2$ and $(0p)^2$ configurations for ^{11}Li using the mixing probabilities of these configurations and the coupling matrix element between them as 0.5 MeV obtained in Ref. [9]. The present model is found to give the degenerated energies enough to couple the $(0p)^2$ and $(1s)^2$ configurations by the pairing interaction.

We calculate the three-body Coulomb breakup strength of ^{11}Li into ^{9}Li+n+n system to investigate the properties of the dipole excited states and compare the strength with the new data from the RIKEN group[4]. We use the Green's function method combining with the complex scaling method to calculate the three-body breakup strength[24] using the dipole strength and the equivalent photon method, where energy resolution is taken into account[4]. We cannot find any resonances with a sharp decay width enough to make a structure in the strength. In Fig. 4, it is found that the present model well reproduces the experiment, in particular, for low energy enhancement and its magnitude.

For the reference, we calculate the strength with a potential model denoted as DR, in which the ^{9}Li core is inert and the ^{9}Li-n s-wave potential is deepened to reproduce 50% of $P(s^2)$ in the ^{11}Li ground state. In this case, we obtain three dipole resonances of $1/2^+$, $3/2^+$ and $5/2^+$ states with $3/2^- \otimes 1^-$, less than 0.5 MeV above the three-body threshold energy, similar to the results of Ref. [8]. In our results, the $3/2^+$ state is located slightly

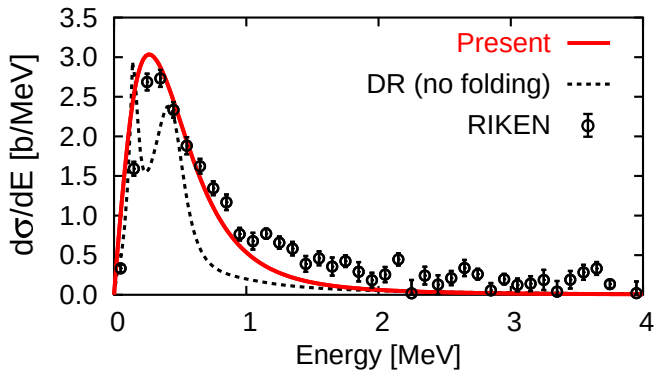

Figure 4: Calculated Coulomb breakup cross section measured from the ^{9}Li+n+n threshold energy.

lower than other two states, which make a visible splitting in the cross section before folding with experimental resolution as shown in Fig. 4.

The charge radius of ^{11}Li was measured recently and its value is 2.467±37 fm, which is enhanced from the one of ^{9}Li, 2.217±35 fm [5]. The present wave functions provide 2.44 fm and 2.23 fm, respectively, which are in good agreement with the experimental values. This enhancement is mainly caused by the large distance between ^{9}Li and the paired two neutrons obtained as 5.69 fm.

4 Summary

We have considered newly the tensor correlation in ^{11}Li based on the extended three-body model. We have found that the tensor and pairing correlations play important roles in ^{9}Li with different spatial characteristics, where the tensor correlation prefers a shrunk spatial extension. The tensor and pairing correlations in ^{9}Li inside ^{11}Li are then Pauli-blocked by additional two neutrons and make the $(1s)^2$ and $(0p)^2$ configurations close to each other and hence activate the pairing interaction to mix about equal amount of two configurations. As a result we naturally explain the breaking of magicity and the halo formation for ^{11}Li. We also reproduce the recent results of the Coulomb breakup strength and the charge radius of ^{11}Li.

References

[1] I. Tanihata *et al.*, Phys. Rev. Lett. **55**, 2676 (1985).

[2] P. G. Hansen and B. Jonson, Europhys. Lett. **4**, 409 (1987).

[3] H. Simon *et al.*, Phys. Rev. Lett. **83**, 496 (1999).

[4] T. Nakamura *et al.*, Phys. Rev. Lett. **96**, 252502 (2006).

[5] R. Sánchez *et al.*, Phys. Rev. Lett. **96**, 033002 (2006).

[6] Y. Tosaka, Y. Suzuki and K. Ikeda, Prog. Theor. Phys. **83**, 1140 (1990).

[7] I. J. Thompson and M. V.Zhukov, Phys. Rev. C **49**, 1904 (1994).

[8] E. Garrido, D. V. Fedorov and A. S. Jensen, Nucl. Phys. **A708**, 277 (2002).

[9] T. Myo, S. Aoyama, K. Katō and K. Ikeda, Prog. Theor. Phys. **108**, 133 (2002).

[10] Y. Akaishi, Int. Rev. of Nucl. Phys. **4**, 259 (1986).

[11] H. Kamada *et al.*, Phys. Rev. C **64**, 044001 (2001).

[12] T. Terasawa, Prog. Theor. Phys. **23**, 87 (1960), Arima and T. Terasawa, Prog. Theor. Phys. **23**, 115 (1960).

[13] S. Nagata, T. Sasakawa, T. Sawada and R. Tamagaki, Prog. Theor. Phys. **22**, 274 (1959).

[14] T. Myo, K. Katō and K. Ikeda, Prog. Theor. Phys. **113**, 763 (2005).

[15] S. Sugimoto, K. Ikeda and H. Toki, Nucl. Phys. **A740**, 77 (2004).

[16] T. Myo, S. Sugimoto, K. Katō, H. Toki and K. Ikeda, Prog. Theor. Phys. **117**, 257 (2007).

[17] Y. Akaishi, Nucl. Phys. **A738**, 80 (2004).

[18] K. Ikeda, S. Sugimoto and H. Toki, Nucl. Phys. **A738**, 73 (2004).

[19] E. Hiyama, Y. Kino and M. Kamimura, Prog. Part. Nucl. Phys. **51**, 223 (2003).

[20] H. Furutani *et al.*, Prog. Theor. Phys. Suppl. **68**, 193 (1980).

[21] S. Aoyama, T. Myo, K. Katō, K. Ikeda, Prog. Theor. Phys. **116**, 1 (2006).

[22] I. Tanihata *et al.*, Phys. Lett. B **206**, 592 (1988).

[23] J. A. Tostevin and J. S. Al Khalili, Nucl. Phys. **A616**, 418c (1997).

[24] T. Myo, S. Aoyama, K. Katō and K. Ikeda, Phys. Lett. B **576**, 281 (2003).